Hindawi
Advances in Civil Engineering
Volume 2022, Article ID 1554204, 9 pages
https://doi.org/10.1155/2022/1554204

Research Article

Influence of Humic Acid on the Strength of Cement-Soil and Analysis of Its Microscopic Mechanism

Jing Cao,[1] Fangyi Liu,[1] Siyang Huang,[1] Cheng Kong,[2] Huafeng Sun,[1] Yue Gao,[3] Fuhua Liu,[4] Jianyun Li,[1] and Guoshou Liu[1]

[1]*Faculty of Civil Engineering and Mechanics, Kunming University of Science and Technology, Kunming 650500, China*
[2]*China Power Construction Group Kunming Survey Design&Research Institute Co.,Ltd, Kunming, China*
[3]*Shenzhen Geotechnical Investigation & Surveying Institute (Group) Co., Ltd, Shenzhen, China*
[4]*Zhejiang Wanning Technology Co., Ltd, Zhejiang, China*

Correspondence should be addressed to Siyang Huang; huangsiyang@stu.kust.edu.cn

Received 29 May 2022; Revised 8 July 2022; Accepted 11 July 2022; Published 8 August 2022

Academic Editor: Navaratnarajah Sathiparan

The disposal of soil containing humic acid (HA) poses an increasingly difficult problem for geotechnical environmental engineering. In this study, the unconfined compressive strength (UCS) test of cement-soil with different HA contents is conducted to analyze the effect of HA on the strength of cement-soil. Mercury intrusion porosimetry (MIP), scanning electron microscopy (SEM), and X-ray diffraction (XRD) experiments reveal the effective mechanism of HA on the strength of cement-soil from the microscopic level. The results show that the strength of cement-soil decreases gradually with the increase of HA content. The failure mode of cement-soil slightly changed from brittle failure to plastic failure. The microscopic test shows that the incorporation of HA will lead to the apparent enlargement of the pores in the cement-soil. The large pores in the sample increase, the small micropores decrease, and the structure tends to be loose and overhead. The increased HA content added will significantly reduce the cement hydration products and destroy the cementation of the hydration products.

1. Introduction

The cement-soil mixing method is a mature technology for the treatment of soft soil foundation, which has the advantages of less impact on the surrounding environment, flexible reinforcement form, and low cost [1–6]. Cement-soil had better strength properties than the original soil [3]. The strength of cement-soil is affected by soil properties, cement mixing content, water content, and curing age [7–10]. The strength of cement-soil is mainly affected by cementing action of cementing material, porosity, and pore size [11].

Peat soil is a special soft soil composed of humic group (HG), soil inorganic matter, animal and plant residues, and it has high organic matter content, high water content, low bearing capacity, large void ratio, low permeability, and high compressibility, [12–14]. HG is an essential part of organic matter in peat soil and a natural organic polymer mixture with a complex structure composed mainly of humic acid (HA), humin, and fulvic acid [15, 16]. Peat soils are widely distributed in China [17]. Since the existence of organic matter can adversely affect the reinforce the soft foundation, it is of great significance to study the effect of HA on the strength of cement-soil for guiding practical engineering.

The research on the effect of HG on cement-soil mostly focuses on the following aspects: Clare et al. [18] added different amounts of organic matter into cement-soil for experiments and found that organic matter would reduce the unconfined compressive strength (UCS) of cement-soil. Kumada [19] found that HA and fulvic acid in soil are the two most representative substances in HG by sorting out the research of related scholars. Shao [20, 21] found that the effect of cement on soil solidification is mainly affected by HA and fulvic acid. Through the UCS test, she studies the influence of HG mass fraction, HA mass fraction, fulvic acid mass fraction, and other factors on HA-containing cement-soil. The results show that HA has a more significant effect

Table 1: Physical properties of soil.

Test soil	Natural moisture content (%)	Liquid limit (%)	Plastic limit (%)	Plasticity index	Natural density ($g{\cdot}cm^{-3}$)	Specific gravity of soil particle (G_s)
Cohesive soil	18.6	39.2	23.0	16.2	1.96	2.73

on the strength of cement-soil than fulvic acid, and HA is having a long-term impact on the strength of cement-soil. Chen and Wang [22] added different amounts of organic matter into cement-soil for related experiments. The test results show that with the increase of organic matter content, the cohesion of cement-soil samples increases slightly, and the internal friction angle decreases obviously, but the shear strength and UCS both decrease. Kang et al. [23] found through related research that HG can affect the formation of cement hydration products and the microstructure of cement-soil. Cao et al. [24] research found that increasing the cement rate can inhibit the effect of HA on cement-soil, and HA can change the microstructure of cement-soil. Consequently, the study of the effect of HA on the strength of cement-soil has been a largely underexplored domain, and there is a lack of microlevel mechanism research.

In this article, the effect of HA on the strength of cement-soil is studied by mixing HA and cement into cohesive soil to form an HA-containing cement-soil. The authors investigated the effect of HA on the strength of cement-soil through unconfined compressive (UCS) test. Scanning electron microscopy (SEM), mercury intrusion porosimetry (MIP), X-ray diffraction (XRD), and other microscopic testing techniques and analytical methods reveal the influence mechanism of HA on the strength of peat soil from the microscopic level.

2. Materials and Methods

2.1. Materials. This experiment uses ordinary Portland cement P.O42.5 produced by Huaxin Cement (Honghe) Co. Ltd. The soil used in the experiment is taken from the vicinity of the student apartment in Jingyuan, Kunming University of Science and Technology, Chenggong District, Kunming City, Yunnan Province. Undisturbed soil is yellow-brown cohesive soil. Table 1 provides the physical properties of the soil tested by a series of tests. Humic acid (HA) reagent is produced by Tianjin Guangfu Chemical Reagent Factory. Combined with the carbon element content of the HA reagent, the pure HA content of the reagent is about 41.68%.

Figure 1 shows the cumulative particle size curve of HA and cohesive soil.

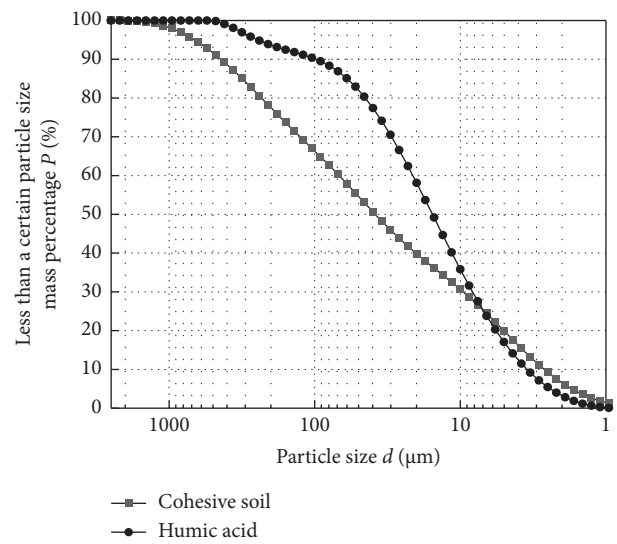

Figure 1: Cumulative particle size curve of test materials.

2.2. Preparation of Samples. The sample preparation is performed according to the "Standards for Geotechnical Test Methods" (GB/T 50123–2019). The cement rate of the cement-soil sample is $\beta = 15\%$, the water-cement ratio $c = 0.5$, the water content $\omega = 24\%$, and the void ratio $e = 0.8$. First, test soil and HA are mashed, dried, passed through 2.00 mm geotechnical sieves, and then packed in boxes for later use. When preparing the sample, a three-lobed mold with an inner diameter of $(d) = 39.10$ mm and a height of $(h) = 80.00$ mm is used as the test mold. After mixing the test soil, HA reagent, and water uniformly, the sample is compacted in three valves by the layered compaction method to ensure that the sample is uniform and dense. The cement-soil samples are sealed with plastic wrap, and after curing in a curing room $(20 \pm 3)^{\circ}$C to a certain strength, they are soaked in distilled water until the design age.

2.3. Testing Program. When cement-soil samples are soaked for the design age, the UCS test, mercury intrusion porosimetry (MIP), scanning electron microscopy (SEM), and X-ray diffraction (XRD) tests are performed on the cement-soil samples. The specific test conditions are given in Table 2. The UCS test adopts the CSS-44000 electronic universal testing machine of Changchun Testing Machine Research Institute. During the test, the axial compression rate of the control instrument is 1.0 mm/min. Cement-soil samples are dried in an oven to constant weight and then subjected to the microstructure test. The author takes 1-2 g samples for the MIP test. MIP test is carried out using the Autopore9510 high-performance automatic mercury porosimeter produced by Micromeritice in the USA [25–27]. The authors collect fingernail-sized samples for SEM experiments. The sample is fixed on the platform with conductive glue and the sample's surface is sprayed with gold and placed in the instrument. SEM test used Czech TESCAN-VEGA3 automatic tungsten filament scanning electron microscope [26, 28]. Before the XRD test, the authors grind the sample into powder and pass it through a 600-

Table 2: Test conditions.

Test method	HA content (λ/%)	Cement rate (β/%)	Water-cement ratio (c)	Water content (w/%)	Void ratio (e)	Soaking time ($/d$)
UCS	0, 5,10, 15, 20, 25, 30	15	0.5	24	0.8	90
SEM, MIP, XRD	0, 10, 20, 30					

mesh test sieve. The XRD test uses the Holland PANalytical X'Pert3 Powder multifunctional powder X-ray diffractometer [29, 30].

3. Analysis of the Effect of Humic Acid on the Strength of Cement-Soil

Figure 2 shows the relationship curve between unconfined compressive strength (UCS) and humic acid (HA) content. Cement-soil UCS decreased gradually with the increase of HA content.

Figure 3 shows the stress-strain curve of the UCS test of cement-soil samples with different HA contents. The stress-strain curves of cement-soil samples with different HA content are the same. All curves have a peak stress intensity, with the increase of axial strain, the stress of the specimen rapidly reaches the peak stress, and then the specimen fails. Its stress decreases and has a certain residual strength (q_{ur}). The UCS of the sample continued to decrease with the increase of HA content, the strain corresponding to UCS increased slightly, and the q_{ur} of the sample decreased slightly. When the HA content is not more than 20%, the stress-strain curve shows the properties of brittle materials. When the HA content is more than 20%, the stress-strain curve tends to be flat, showing prominent properties of plastic materials.

Figure 4 shows the compression failure form and failure surface images of cement-soil. When the cement-soil without HA is damaged, cracks run through the top and bottom, showing the phenomenon of brittle failure. The cement-soil samples gradually show plastic failure with the increase of HA content. With the addition of HA, the failure surface color gradually changed from yellowish-brown to dark brown.

With the increase of HA content, HA particles gradually replaced part of clay mineral soil particles to become the skeleton of cement-soil. Compared with other inorganic minerals in the soil, HA agglomerates have higher compressibility, so the compressive capacity of cement-soil with HA as a skeleton is weak [12, 31]. HA particles are smaller than most clay mineral soil particles and usually have a negative charge, which makes HA particles adsorb on the surface of cement and clay particles, hindering the interaction between cement and clay mineral soil particles, resulting in cement-soil strength reduction [32]. HA disperses clay particles, hinders the coagulation between clay particles, and weakens the cementation effect of cement hydration reaction to soil particles [33].

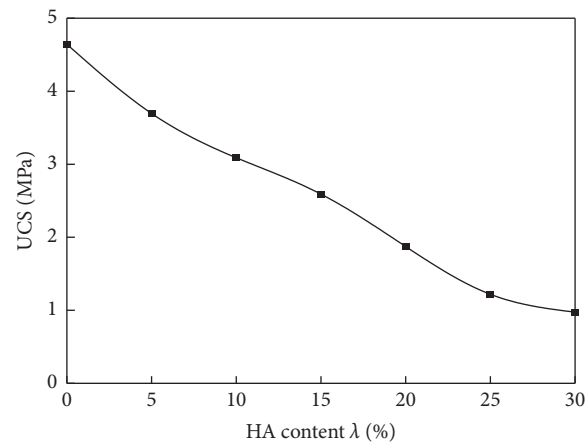

Figure 2: The relationship between UCS and HA content λ in cement-soil.

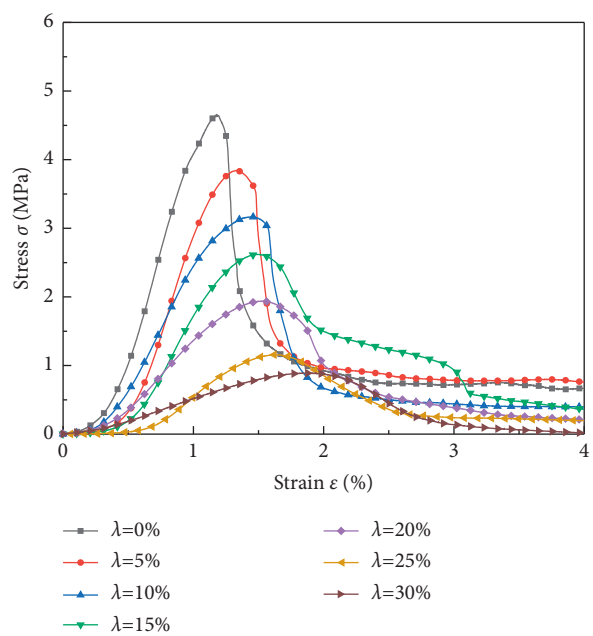

Figure 3: Stress-strain curves of cement-soil and samples UCS with different HA content λ.

4. Microscopic Test Results and Mechanism Analysis

4.1. Mercury Intrusion Test Results and Analysis. Figure 5 shows cement-soil samples' pore distribution curve under

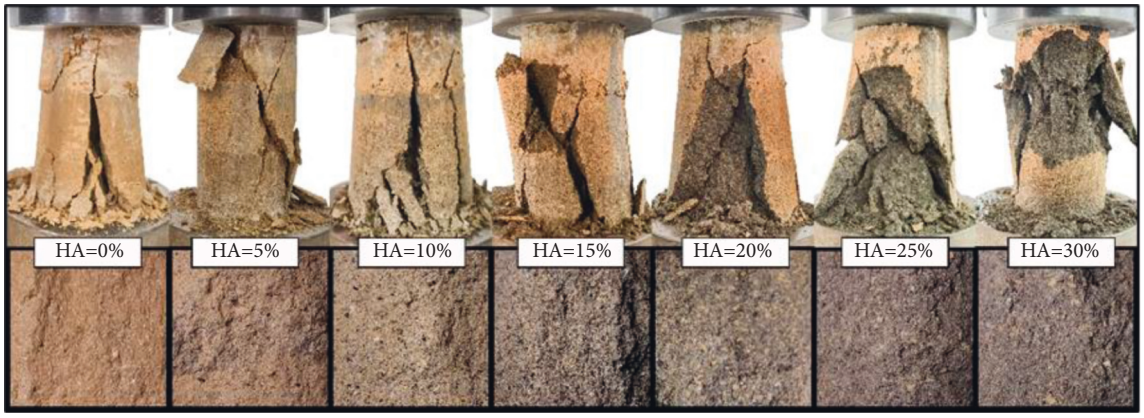

Figure 4: Cement-soil failure form and failure surface.

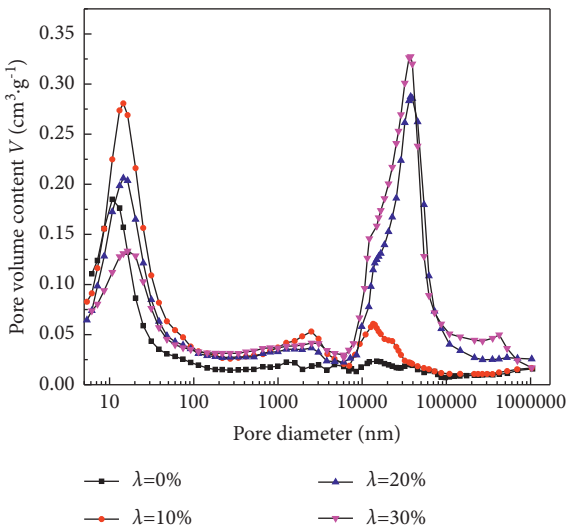

Figure 5: Pore distribution of cement-soil samples with different HA content λ.

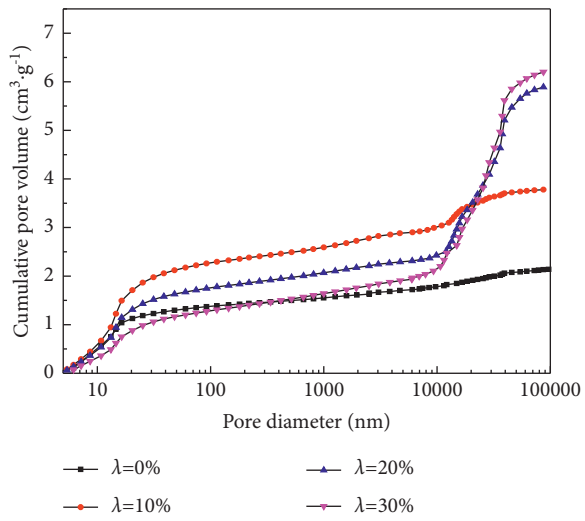

Figure 6: Pore accumulation curve of cement-soil samples with different HA content λ.

different humic acid (HA) contents. To facilitate the analysis, according to the curve characteristics shown Figures 5 and 6, the pores can be divided into four types according to the pore size of the pores inside the cement-soil sample: large pores, pore size $d > 10000$ nm; mesopores, pore size $100\,\text{nm} < d < 10000\,\text{nm}$; small pores, pore size $10\,\text{nm} < d < 100\,\text{nm}$; and micropores, pore size $d < 10$ nm.

According to the test results, the following characteristics are obtained: according to the pore distribution curve, the pore size distribution of cement-soil samples without HA has a unimodal structure. In contrast, the pore size distribution of cement-soil samples doped with HA has a bimodal structure. The pore size of cement-soil gradually increased with the increase of HA content, from a structure dominated by small micropores to a structure dominated by macropores.

Figure 6 shows cement-soil samples' pore accumulation curve with different HA content. The total pore volume increases gradually with the incorporation of HA, the sample structure tends to be loose, and the pore connectivity increases.

According to the Powers [34–37] theory, as the hydration reaction proceeds, the volume fraction of hydration products increases, reducing the sample's pore volume. Increasing OH^- ion concentration during cement hydration reaction will increase the pH value [38]. HA is soluble in dilute alkaline solution, partially dissolves HA particles during soaking, increasing pore volume [39].

Table 3 provides pore size distribution data of cement-soil with different HA contents. The volume of macropores increases significantly when the HA content is more significant than 10%. With the increase of HA in the cement-soil, the small pores gradually decreased, and the mesopores increased slowly.

According to Figure 1, the particle size of the HA reagent is between 10,000 and 100,000 nm, accounting for nearly 50%. With the dissolution of the HA particles, large pores are formed inside the cement-soil mixed with HA. The HA particles gradually become cement-soil skeleton when the HA content is from 10% to 20%. HA particles have different degrees of connection. The dissolution of HA particles enhances the pore connectivity in cement-soil. The dissolution of HA particles increases macropore volume in

Table 3: Pore size distribution of cement-soil with different HA content λ.

Sample	Average pore size (d/nm)	Pore volume in different pore size ranges/($cm^3 \cdot g^{-1}$)			
		Large pores, $d > 10000$ nm	Mesopores, $100\ nm < d < 10000\ nm$	Small pores, $10\ nm < d < 100\ nm$	Micropores, $d < 10$ nm
$\lambda = 0\%$	23.9	0.49	0.41	0.98	0.39
$\lambda = 10\%$	23.3	0.92	0.73	1.81	0.45
$\lambda = 20\%$	39.9	3.72	0.68	1.38	0.37
$\lambda = 30\%$	59.8	4.46	0.83	1.03	0.25

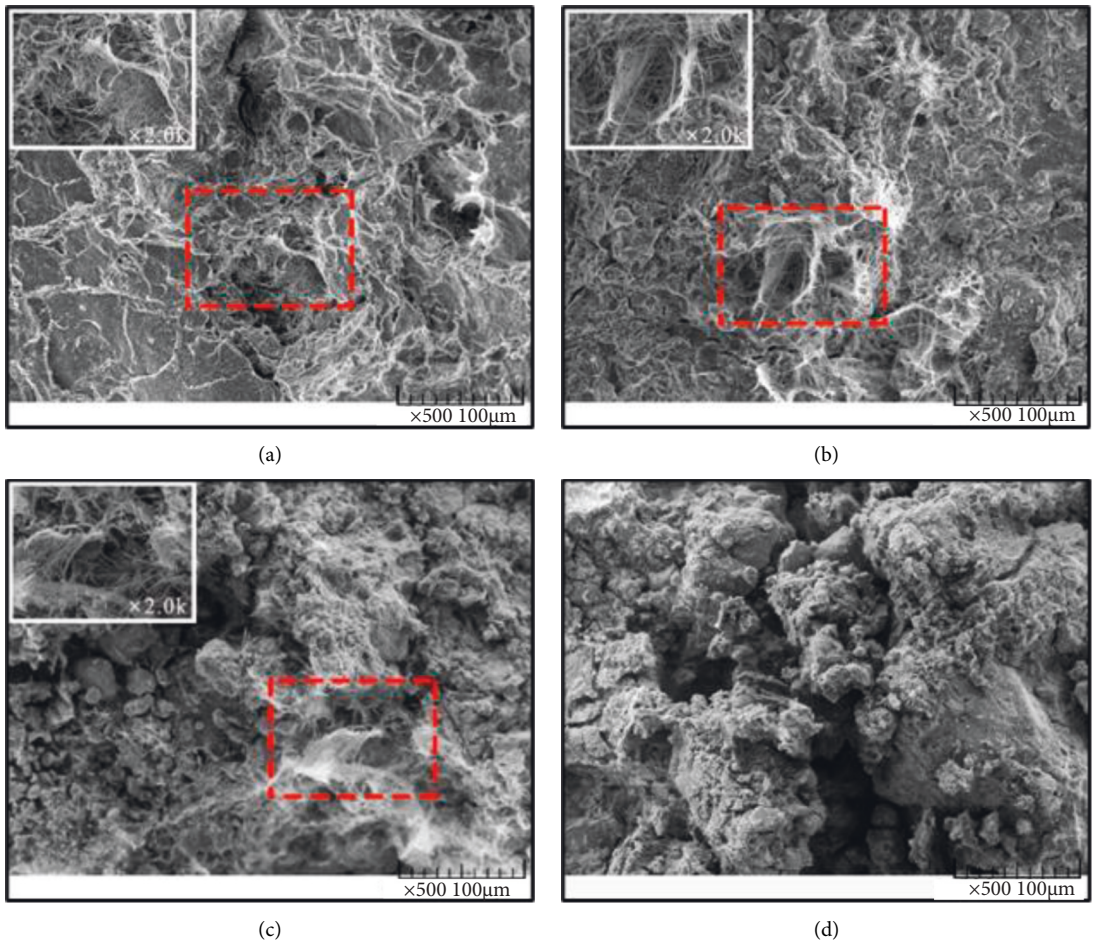

Figure 7: Microstructure images of different samples. (a) HA content $\lambda = 0\%$. (b) HA content $\lambda = 10\%$. (c) HA content $\lambda = 20\%$. (d) HA content $\lambda = 30\%$.

cement-soil. The solubility limit of HA resulted in little change in macropores when the HA content is from 20% to 30%.

4.2. Scanning Electron Microscopy Results and Analysis. Figure 7 shows the scanning electron microscopy (SEM) images of 500 times and 2000 times magnification of cement-soil with HA content of 0%, 10%, 20%, and 30%. According to the image analysis, the following rules can be drawn: it can be seen from Figure 7(a) that the microstructure of the cement-soil without HA is relatively dense and uniform. Cement hydration products and crystals connect the clay particles, and the particles become larger structural units through cementation, less large pores. It can be seen from Figure 7(a) that the microstructure of the cement-soil without HA is relatively dense and uniform. Cement hydration products and crystals connect the clay particles, and the particles become larger structural units through cementation, less large pores. The crystals produced by the hydration reaction increase the volume of the solid phase in the cement-soil, making the soil structure denser [40]. Calcium silicate hydrate (C-S-H, $6CaO \cdot 5SiO_2 \cdot 6H_2O$) is widely distributed and is fibrous or reticular, and acicular ettringite crystals can be seen locally throughout the particles

[36, 41]. The formation of hydration products reflects the strong alkalinity in the internal environment of the sample. It can be seen from Figures 7(b)–7(d) that with the increase of HA content, the pores of cement-soil samples become larger obviously, the large pores around the particles become more, and the connectivity is enhanced. The degree of particle cementation becomes poor, forming a loose overhead skeleton. The experimental phenomenon is consistent with the mercury intrusion porosimetry (MIP) results. The addition of HA can increase the large pore volume of the sample, reduce the degree of cementation and density uniformity, and decrease its unconfined compressive strength (UCS). The network structure of hydration products tended to be sparse with the increase in HA incorporation. When the HA content is 30%, the hydration products are less, and there are no apparent hydrated calcium silicate and ettringite crystals under 500 times magnification. High HA content will affect cement hydration reaction.

Cement hydration products constitute the cement-soil strength's central part [42]. C-S-H is the main hydration product of ordinary Portland cement [43]. According to the related article, C-S-H has the following thermodynamic equilibrium [44]:

$$6Ca^{2+} + 5HSiO_3^- + 7OH^- \rightleftharpoons 6CaO \cdot 5SiO_2 \cdot 6H_2O. \quad (1)$$

It can be seen from the thermodynamic equilibrium formula of C-S-H that the reduction of Ca^{2+} and OH^- will reduce the generation of C-S-H. HA can form insoluble salts with multivalent cations generated by the hydration reaction, which affects the formation of crystalline hydration products [45]. HA has a strong chemical affinity for Ca^{2+}. HA and Ca^{2+} form an insoluble salt called calcium HA. The formation of calcium HA decreases the cement hydration products and affects the strength of cement-soil [21]. The addition of HA destroys cement's cementation and skeleton effect in the original soil and weakens the connection between soil particles [46]. In conclusion, HA inhibits forming of hydration products such as calcium silicate hydrate, calcium aluminate hydrate, and ettringite, weakening the cement-soil solidification effect and decreasing cement-soil strength.

4.3. X-Ray Diffraction Analysis. Using Jade 6.0 software as the analysis software for the X-ray diffraction test results, the test curve peak is compared with the card peak intensity. Figure 8 shows the X-ray diffraction pattern of the cohesive soil. It can be seen from Figure 8 that the main components in the cohesive soil are as follows: original mineral: quartz (SiO_2); secondary mineral: kaolinite ($Al_2O_3{\cdot}2SiO_2{\cdot}2H_2O$) and mica ($KAl_2(AlSi_3O_{10})(OH)_2$); and hydration products: calcium silicate hydrate (C-S-H) and tobermorite ($Ca_5Si_6O_{16}(OH)_2{\cdot}8H_2O$).

The existence of a crystal structure for HA is inconclusive and therefore not analyzed [34]. According to the relevant research results of scholars [47–50], the XRD characteristic peaks (2θ) of the calcium silicate hydrate gel are 29.1°, 31.8°, 49.8°, and 54.9°, respectively. The XRD characteristic peaks (2θ) of the hydration product table mullite crystal

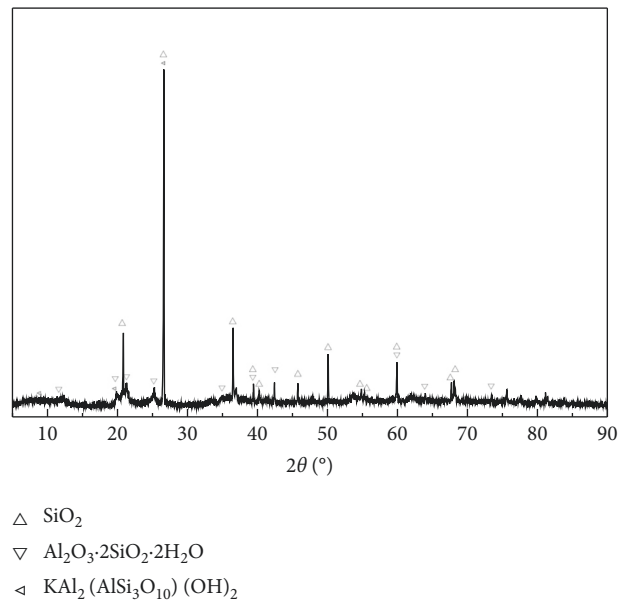

Figure 8: XRD patterns of cohesive clay.

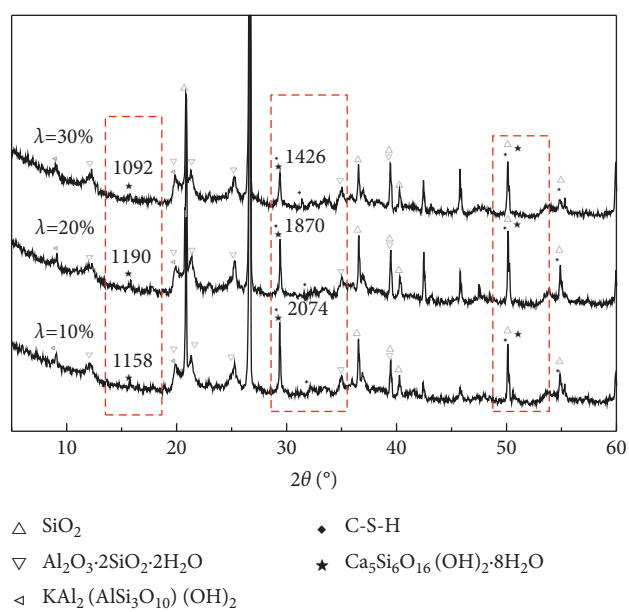

Figure 9: XRD patterns of cement-soil with different HA content λ.

($Ca_5Si_6O_{16}(OH)_2{\cdot}8H_2O$) are 16.1°, 29°, and 49.6°, respectively. Jade6.0 software analyzes the X-ray diffraction test results of cement-soil samples. It is found that the XRD characteristic peak (2θ) of cement hydration products (hydrated calcium silicate gel and tobermorite crystal) is about 29.1°. The test results agree with the research results of related scholars, so this article selects 29.1° as the hydration product's XRD characteristic peak (2θ). From Figure 9, it can be concluded that with the increase of HA content, the characteristic peak heights of cement hydration products (hydrated calcium silicate gel and tobermorite crystal) decreased significantly, and the content is significantly

reduced. From Figure 9, it can be concluded that with the increase of HA content, the characteristic peak height of cement hydration products (hydrated calcium silicate gel and tobermorite crystal) decreased significantly, and the content is significantly reduced. Therefore, HA has an inhibitory effect on the formation of cement hydration products, which eventually leads to a significant weakening effect of HA on the strength of cement-soil samples.

5. Conclusions

In this study, unconfined compressive strength (UCS) tests and microscopic tests are carried out on cement-soil with different humic acid (HA) content. Based on the microscopic tests to study the mechanism of the effect of HA on cement-soil, the following conclusions are drawn:

(1) The UCS test showed that with the increase of HA content, HA particles gradually replaced some clay mineral soil particles to become the skeleton of cement-soil, and the UCS of cement-soil decreased gradually. The addition of HA changed the mechanical properties of cement-soil, and the failure mode gradually changed from brittle failure to plastic failure.

(2) Mercury intrusion porosimetry (MIP) and scanning electron microscopy (SEM) showed that the increase of HA content made the cement-soil pores larger. The pore volume increases and has certain connectivity. The alkaline environment created by the cement hydration reaction can dissolve some HA particles, aggravating the cement-soil looseness and weakening the cement's solidification.

(3) X-ray diffraction (XRD) experiments showed that the peak intensity of hydration products decreased significantly with the increased HA content. The content of hydration products decreased. HA has an inhibitory effect on the formation of cement hydration products, resulting in the weakening of the strength of cement-soil.

(4) Combined with the microscopic test results, the effect of HA on the strength of cement-soil is mainly reflected in two aspects. On the one hand, HA inhibits the formation of hydration products. The addition of HA will change the physical and chemical properties of cohesive clay particles, delay the progress of cement hydration reaction, and reduce hydration products. On the other hand, HA will increase the pore volume of the cement-soil. Cement-soil pores become larger, pore connectivity is enhanced, and the structure tends to be loose and overhead. Finally, the cement-soil strength decreased gradually with the increase of HA content.

(5) The comprehensive test results show that HA can significantly reduce the strength of cement-soil, but increasing the cement rate can effectively inhibit the effect of HA. The test results are as expected. Based on previous research, this article discusses the strength development law and microstructure change of HA on cement-soil from a microscopic perspective. The effect of humic acid on cement-soil and the microscopic mechanism is proved. Comparing the strength change law and microstructure test, adding cement into peat soil can appropriately reduce the influence of HA. However, the presence of HA will still weaken cement's hydration reaction and change cement-soil's internal microstructure. In future research and actual engineering of the peat soil environment in the Dianchi Lake area, a more reasonable and effective method to improve the mechanical properties of cement-soil in the peat soil environment can be explored based on the conclusions of this article. Because HG is not only composed of HA, the influence of other substances in HG on the engineering properties of cement needs to be further discussed.

Data Availability

The data used to support the finding of this study are included within the article.

Conflicts of Interest

The authors declare that they have no conflicts of interest.

Acknowledgments

This study was supported by the Natural Science Foundation of China (Yunnan Province) (41967035).

References

[1] X. Gong, *Foundation Treatment Manual [M]*, China Construction Industry Press, 2008.

[2] Jgj 79-2012, "Technical specification for Building Foundation treatment [S]," 2012.

[3] H. Chen, L. Li, J. Li, and De'an Sun, "A generic analytical Elastic solution for Excavation Responses of an Arbitrarily shaped Deep Opening under Biaxial in situ stresses," *International Journal of Geomechanics*, vol. 22, no. 4, Article ID 04022023, 2022.

[4] H. Chen and L. Zhang, "A machine Learning-based method for Predicting End-bearing capacity of Rock-socketed shafts," *Rock Mechanics and Rock Engineering*, vol. 55, no. 3, pp. 1743–1757, 2022.

[5] H. Chen, H. Zhu, and L. Zhang, "A three-Dimensional (3D) semi-analytical solution for the Ultimate End-bearing capacity of Rock-socketed shafts," *Rock Mechanics and Rock Engineering*, vol. 55, no. 2, pp. 611–627, 2022.

[6] G. Tao, X. Wu, X. Yang, W. Liu, J. He, and Y. Chen, "Pore distribution of cement-soil and its influence on permeability [J]," *Chinese Journal of Engineering Geology*, vol. 26, no. 05, pp. 1243–1249, 2018.

[7] C. Chu, Z. Hong, S. Liu, and T. Xu, "Prediction of unconfined compressive strength of soil-cement using water-cement ratio [J]," *Geotechnical Mechanics*, vol. 26, no. 04, pp. 645–649, 2005.

[8] R. Liang, M. Zhang, and X. Bai, "Experimental study on mechanical properties of cement soil[J]," *Geotechnical Mechanics*, vol. 22, no. 2, p. 3, 2001.

[9] S. Liu, G. Qian, and D. Zhang, *Theory and Engineering Application of Powder-Jet Pile Composite Foundation [M]*, China Building Industry Press, 2006.

[10] F. Zhang, C. Huang, T. Yao, and M. Yang, "Experimental study on laws of compression and rebound deformation of peaty soil[J]," *Chinese Journal of Geotechnical Engineering*, vol. 43, no. S2, pp. 259–262, 2021.

[11] Y. Xun, "Experimental study on the reinforcement of soft soil with cement-based curing agent containing industrial waste [J]," *Chinese Journal of Geotechnical Engineering*, vol. 22, no. 02, pp. 210–213, 2000.

[12] S. Gowthaman, M. Chen, K. Nakashima, S. Komatsu, and S. Kawasaki, "Biocementation technology for stabilization/solidification of organic peat," in *Low Carbon Stabilization and Solidification of Hazardous Wastes*, pp. 49–64, Elsevier, 2022.

[13] J. Huang, "Improvement Measures of support and water-stop pile in peat soil[J]," *Chinese Journal of Underground Space and Engineering*, vol. 12, no. S2, pp. 739–742, 2016.

[14] J. Yang, T. Sun, Y. Zhang, and J. Miao, "Deterioration of soil cement stabilized in corrosive site[J]," *Chinese Journal of Geotechnical Engineering*, vol. 34, no. 01, pp. 130–138, 2012.

[15] B. Yang, *Research on Strength Law of Cement and Soil [D]*, Shanghai Jiaotong University, 2007.

[16] Y. Gui, Z. Yu, H. Liu, J. Cao, and Z. Wang, "Analysis of secondary consolidation characteristics and mechanism of plateau lacustrine peat soil[J]," *Chinese Journal of Geotechnical Engineering*, vol. 37, no. 08, pp. 1390–1398, 2015.

[17] X. Ma, *China's Peatland Carbon Storage and Carbon Emissions [M]*, China Forestry Press, Beijing, 2013.

[18] K. E. Clare and P. T. Sherwood, "The effect of organic matter on the setting of soil-cement mixtures[J]," *Journal of Chemical Technology and Biotechnology*, vol. 4, no. 11, pp. 625–630, 1954.

[19] K. Kumada, *Chemistry of Soil Organic matter[M]*, Elsevier, 1988.

[20] Y. Shao, X. Gong, R. Xu, and Z. Liu, "Research progress on the effect of organic matter on the reinforcement effect of soil stabilizers[J]," *Agricultural Mechanization Research*, vol. 27, no. 01, pp. 23-24+27, 2005.

[21] Y. Shao, X. Gong, R. Xu, and Z. Liu, "Effect of humic acid on the strength of cement and soil[J]," *Journal of Jiangsu University(Natural Science Edition)*, vol. 28, no. 04, pp. 354–357, 2007.

[22] H.'e Chen and Q. Wang, "Influence of organic matter on the effect of cement reinforcement on soft soil [J]," *Chinese Journal of Rock Mechanics and Engineering*, vol. 24, no. 202, pp. 5816–5821, 2005.

[23] G. o Kang, T. Tsuchida, Y. s Kim, and Wj Baek, "Influence of humic acid on the strength Behavior of cement-Treated clay during Various curing stages," *Journal of Materials in Civil Engineering*, vol. 29, no. 8, Article ID 04017057, 2017.

[24] J. Cao, S. Huang, W. Liu, Y. Gao, Y. Song, and S. Li, "Study on strength development and microstructure of cement-solidified peat soil containing humic acid of Dianchi Lake[J]," *Advances in Materials Science and Engineering*, vol. 2022, Article ID 8136852, 2022.

[25] A. B. Abell, K. L. Willis, and D. A. Lange, "Mercury intrusion porosimetry and image analysis of cement-based materials," *Journal of Colloid and Interface Science*, vol. 211, no. 1, pp. 39–44, 1999.

[26] *A Practical Guide to Microstructural Analysis of Cementitious materials[M]*, Crc Press, Boca Raton, FL, USA, 2016.

[27] H. Ma, "Mercury intrusion porosimetry in concrete technology: tips in measurement, pore structure parameter acquisition and application," *Journal of Porous Materials*, vol. 21, no. 2, pp. 207–215, 2014.

[28] J. N. T. Nguyen and A. M. Harbison, "Scanning electron microscopy sample preparation and imaging," *Methods in Molecular Biology*, vol. 1606, pp. 71–84, 2017.

[29] D. M. Moore and R. C. Reynolds Jr, *X-ray Diffraction and the Identification and Analysis of Clay Minerals[M]*, Oxford University Press, 1989.

[30] D. L. Bish and J. E. Post, *Modern Powder diffraction[M]*, Walter de Gruyter GmbH & Co KG, 2018.

[31] F. J. Stevenson, *Humus Chemistry: Genesis, Composition, reactions[M]*, John Wiley & Sons, 1994.

[32] C. Lin, *Soil Science (Northern Edition) [M]*, Agricultural Press, Beijing, 1983.

[33] Y. Lan, Q. Hu, and J. Xue, "Effects of humic acid on soil and mineral clay dispersion [J]," *Soil Journal*, vol. 35, no. 2, pp. 195–201, 1998.

[34] T. C. Powers, "Studies of the physical properties of Hardened Portland cement Pastes[J]," *International Concrete Abstracts Portal*, vol. 43, pp. 249–336, 1948.

[35] H. F. W. Taylor, *Cement chemistry[M]*, Thomas Telford, London, 1997.

[36] P. K. Mehta and P. J. M. Monteiro, *Concrete: Microstructure, Properties, and materials[M]*, McGraw-Hill Education, 2014.

[37] H. M. Jennings, "A model for the microstructure of calcium silicate hydrate in cement paste," *Cement and Concrete Research*, vol. 30, no. 1, pp. 101–116, 2000.

[38] D. L. Richman, C. L. Tucker, and P. G. Koehler, "Influence of Portland cement amendment on soil pH and residual soil termiticide performance," *Pest Management Science*, vol. 62, no. 12, pp. 1216–1223, 2006.

[39] Q. Wen, *Soil Organic Matter Research Method [M]*, Agricultural Press, Beijing, 1984.

[40] Y. Dong, Q.'e Zhang, R. Xu, and X. Gong, "Experimental study on the effect of curing agent on the strength of soft soil [J]," *Rock and Soil Mechanics*, vol. 29, no. 02, pp. 475–478, 2008.

[41] J. Wu, H. Jing, Y. Gao, Q. Meng, Q. Yin, and Y Du, "Effects of carbon nanotube dosage and aggregate size distribution on mechanical property and microstructure of cemented rockfill," *Cement and Concrete Composites*, vol. 127, p. 104408, Article ID 104408, 2022.

[42] X. Huang and G. Zhou, "A preliminary study on the hardening mechanism of cement-reinforced soil [J]," *Chinese Journal of Rock Engineering*, vol. 16, pp. 62–68, 1994.

[43] W. Zhang, H. Wang, and J. Ye, "The structure and changes of calcium silicate hydrate [J]," *Journal of Silicate*, vol. 33, no. 1, pp. 63–68, 2005.

[44] K. Suzuki, T. Nishikawa, and S. Ito, "Formation and carbonation of C-S-H in water," *Cement and Concrete Research*, vol. 15, no. 2, pp. 213–224, 1985.

[45] J. Cao, D. Yuan, and G. Pan, "Soil in Karst Ecosystem[J]," *Advances in Earth Science*, vol. 18, no. 1, pp. 37–44, 2003.

[46] Y. Gao and J. Zheng, "Indoor experimental study of cement and soil [J]," *Journal of Hohai University (Natural Science Edition)*, vol. 27, no. 5, pp. 103–106, 1999.

[47] Ya Dong, C. Lu, Y. Ni, and Z. Xu, "Study on morphology control and drug loading performance of mesoporous calcium silicate hydrate microspheres [J]," *Bulletin of Silicate*, vol. 31, no. 3, pp. 511–515, 2012.

[48] Y. Wang, Q. Zhao, and S. Zhou, "The effect of temperature on the microstructure of calcium silicate hydrate synthesized by solution method [J]," *Bulletin of Silicate*, vol. 37, no. 9, pp. 2817–2821, 2018.

[49] Y. Lei, T. Han, H. Wang et al., "Preparation and characterization of hydrothermally synthesized calcium silicate hydrate (C-S-H)[J]," *Silicate Bulletin*, vol. 33, no. 03, pp. 465–469, 2014.

[50] M. Zhang and J. Chang, "Surfactant-assisted sonochemical synthesis of hollow calcium silicate hydrate (CSH) microspheres for drug delivery," *Ultrasonics Sonochemistry*, vol. 17, no. 5, pp. 789–792, 2010.